

Battery choice and management for New Generation Electric Vehicles

*Original*

Battery choice and management for New Generation Electric Vehicles / A., Affanni; A., Bellini; G., Franceschini; Guglielmi, Paolo; C., Tassoni. - In: IEEE TRANSACTIONS ON INDUSTRIAL ELECTRONICS. - ISSN 0278-0046. - 52:5(2005), pp. 1343-1349. [10.1109/TIE.2005.855664]

*Availability:*

This version is available at: 11583/1503806 since:

*Publisher:*

IEEE

*Published*

DOI:10.1109/TIE.2005.855664

*Terms of use:*

This article is made available under terms and conditions as specified in the corresponding bibliographic description in the repository

*Publisher copyright*

(Article begins on next page)

# Battery Choice and Management for New-Generation Electric Vehicles

Antonio Affanni, Alberto Bellini, *Member, IEEE*, Giovanni Franceschini, Paolo Guglielmi, and Carla Tassoni, *Senior Member, IEEE*

**Abstract**—Different types of electric vehicles (EVs) have been recently designed with the aim of solving pollution problems caused by the emission of gasoline-powered engines. Environmental problems promote the adoption of new-generation electric vehicles for urban transportation. As it is well known, one of the weakest points of electric vehicles is the battery system. Vehicle autonomy and, therefore, accurate detection of battery state of charge (SoC) together with battery expected life, i.e., battery state of health, are among the major drawbacks that prevent the introduction of electric vehicles in the consumer market. The electric scooter may provide the most feasible opportunity among EVs. They may be a replacement product for the primary-use vehicle, especially in Europe and Asia, provided that drive performance, safety, and cost issues are similar to actual engine scooters.

The battery system choice is a crucial item, and thanks to an increasing emphasis on vehicle range and performance, the Li-ion battery could become a viable candidate. This paper deals with the design of a battery pack based on Li-ion technology for a prototype electric scooter with high performance and autonomy. The adopted battery system is composed of a suitable number of cells series connected, featuring a high voltage level. Therefore, cell equalization and monitoring need to be provided. Due to manufacturing asymmetries, charge and discharge cycles lead to cell unbalancing, reducing battery capacity and, depending on cell type, causing safety troubles or strongly limiting the storage capacity of the full pack.

No solution is available on the market at a cheap price, because of the required voltage level and performance, therefore, a dedicated battery management system was designed, that also includes a battery SoC monitoring. The proposed solution features a high capability of energy storing in braking conditions, charge equalization, overvoltage and undervoltage protection and, obviously, SoC information in order to optimize autonomy instead of performance or vice-versa.

**Index Terms**—Batteries, electric vehicles (EVs).

## I. INTRODUCTION

**B**ATTERIES for high-performances electric vehicles (EVs) should be a nice tradeoff between “drive performance” and “high reliability.” The former feature includes vehicle autonomy and power output, and the latter includes a long lifetime, a maintenance-free system, high degree of safety, and energy regeneration capabilities. In order to achieve these goals the following characteristics are required for an ideal

battery for an EV: high energy density, high output power (density), long life, high charge–discharge efficiency, wide range of use from low temperature to high temperatures, minimal self-discharge, good load characteristics, good temperature storage characteristics, low internal resistance, no memory effects, fast charging, high degree of safety, high reliability, low cost, and good recycleability, [1], [2].

Electric scooters, which address the “drive performance” issue, may provide a more feasible opportunity for Li-Ion battery technology. Thanks to an increasing emphasis on vehicle range and battery energy density, Li-ion could become a viable candidate and, unlike nonelectric vehicles (NEVs) and electric-assisted bicycles, electric scooters may be a replacement product for primary-use vehicles, especially in Europe and Asia. Lithium-ion rechargeable batteries are gaining popularity over nickel-based rechargeable batteries, as the Li-ion characteristics are very attractive and unique. The greatest advantages are the high cell voltage (3 : 1 compared with nickel technology) and superior energy density (roughly, 2 : 1). Other attractive features are a very low self-discharge rate (about 1 : 4 compared with nickel technology) and no memory effect. However Li-ion batteries are much less tolerant of abuse than nickel-based chemistries. Overcharging and overdischarging greatly reduces cycle life. Worse yet, depending on cathode chemistry overcharging may cause battery overheating, venting, or even explosions. The overcharge voltage is within a few percent of the desired full-charge voltage, requiring accurate voltage monitoring during charge to distinguish between full charge and overcharge [3].

In order to address this safety issue, battery protection circuits must be properly designed and included within the Li-ion batteries. The circuitry is designed into the battery “pack” and is normally transparent to the user. Its purpose is to monitor the battery cell voltages and to prevent overcharge or overdischarge by opening the current path if a cell is out of the normal operating voltage range. Overload and short-circuit protection is also provided, monitoring the discharge current and opening the circuit if the current exceeds a pre determined threshold. There are many challenges in designing a practical battery protection circuit. It must be small and economical enough for the manufacturer to include it inside the battery pack. Moreover, in order to minimize impact on battery life, the circuit’s current consumption must be significantly lower than the inherent self-discharge rate of the battery, since it is powered continuously. The cell voltage monitoring circuit must be very accurate to allow a full charge while preventing an overcharge. If the overcharge threshold is too low, it will prevent the battery from

Manuscript received June 3, 2004; revised November 18, 2004. Abstract published on the Internet July 15, 2005. This work was supported by the Italian Government under COFIN 2000. This paper was presented at the 2003 IEEE International Electric Machines and Drives Conference, Madison, WI, June 1–4.

A. Affanni, A. Bellini, G. Franceschini and C. Tassoni are with the Department of Information Engineering, University of Parma, 43100 Parma, Italy.

P. Guglielmi is with the Department of Electrical Engineering, Politecnico di Torino, 10129 Turin, Italy.

Digital Object Identifier 10.1109/TIE.2005.855664

TABLE I  
SINGLE CELL VERSUS BATTERY PACK

PARAMETER	CELL	BATTERY
Chemistry	LiCoO <sub>2</sub>	LiCoO <sub>2</sub>
Typ. Voltage	3.7V	260V+260V
Minimum Capacity	10Ah	10Ah+10Ah
Minimum Energy Density	105 Wh/Kg	105 Wh/Kg
Max Dis/Charge Current	30A/20 °	30A/20A
Cycle Life (minimum)	500 cycles C	500 cycles C
Initial Internal Impedance	≤ 6m Ω	≤ 350m Ω
Cell Weight	≤ 350g	≤ 49 Kg
Discharge Temperature	-20 60 °C	-20 60 °C

being fully charged, reducing operating time between charges. If the threshold is too high, the battery may be damaged by an overcharge [4]–[6]. In order to store the maximum amount of energy, charge equalization of every cell would be required, and it becomes mandatory in the case of cell imbalance due to intrinsic manufacturing differences or repeated charge/discharge cycles. Toward this aim, suitable equalization circuits must be added for every single cell.

## II. BATTERY PACK DESIGN

The developed battery pack consists of two independent batteries parallelly connected through two dc/dc converters to a common dc link. Each battery is constituted of 70 LiCoO<sub>2</sub> cells series connected for a nominal battery voltage of about 260 V. Table I reports the characteristics of a single cell and of the whole battery pack. Fig. 1 shows the battery stack: seven packs connected in series constitute the two batteries. The ten cells inside every pack are individually protected and equalized by a suitable electronic circuit.

As is known, charge and discharge cutoffs for the lithium-ion battery cells must be closely controlled or early cell damage will occur: Overcharge leads to electrolyte oxidation and decomposition while overdischarge results in cathode structural changes. The high number of adopted cells (70) stacked in series compounds the problem: under these conditions individual cell monitoring and equalization must be provided.

### A. Cell Voltage Monitoring

According to manufacturer specifications the cell charge must be stopped if voltage exceeds 4.2 V and, additionally, cell discharge will be stopped if cell voltage falls below the 2.7-V threshold. Obviously, from the energy storage point of view, stopping battery charge when the first cell surpasses the voltage threshold is not an efficient solution. This would result in storing an amount of energy clamped by the leakiest cell of the stripe. In order to optimize EV autonomy, a proper charge equalization must be provided. In fact, the voltage profile during discharge may be remarkably different for each cell within a ten-cell stripe battery pack.

The cell voltage monitoring circuit consists of a precision temperature compensated voltage reference and of a resistor voltage divider to sense cell voltage. The voltage of each cell

is continuously compared with voltage reference to state cell voltage condition. Suitable threshold hysteresis was implemented for both overvoltage and undervoltage conditions to prevent oscillation due to battery equivalent series resistance (ESR). Parasitic elements must be taken into account during transient conditions because voltage drop can deceive the protection circuit causing false undervoltage. RC low-pass filters with suitably large time constant were used to address this issue. Dedicated circuits were designed for overvoltage and undervoltage monitoring. High resistance values were used in order to decrease power consumption. Moreover, resistance tolerance is very important to achieve accurate protection: SMD resistors 0805 series with 0.5% tolerance values were used extensively. The normal operating voltage range of each cell is [3 V, 4.15 V]. When the voltage exceeds this range, undervoltage and overvoltage protection circuits start to operate, sending the actual cell voltage level to the control by an optocoupler. Specifically, in the overvoltage operation range [4.15 V, 4.25 V], the overvoltage circuit produces a linear voltage depending on the charge state of the relevant cell.

With a dual behavior in the undervoltage operation range [2.7 V, 3 V], the undervoltage circuit produces a linear voltage depending on the charge state of the relevant cell. When two or more cells are operating in a nonoptimal voltage, the control board acts as an ex-or and sends the output of the sensing circuit which shows the worst case of charge state. A temperature sensor ensures that the battery pack temperature does not surpass 70 °C, in order to prevent damage to the cells. The outputs of the above-mentioned protection circuits are sent through a proper interface (implemented with an array of optocouplers) to the motion control digital signal processor (DSP) allowing a tuning control strategy according to journey characteristics. Each sensor observes the voltage across the relevant cell independently of the position of the cell inside the pack. The reason for the different slopes between overvoltage and undervoltage transitions is due to the different priority of intervention. In overvoltage conditions, the DSP must stop the charge at constant current starting the charge at constant voltage. On the other hand, when a cell is in undervoltage condition the DSP must reduce the current requested by the user providing less acceleration in order to guarantee the best autonomy of the vehicle and allowing a larger margin of battery safety.

### B. Cell Equalization

To obtain maximum energy storage, cells must be individually equalized during charge operation. Toward this aim, in the literature several solutions are adopted. The most widely used are critically reviewed in Table II.

In spite of higher energy efficiency, the use of reactive switched elements was discarded because it leads to a bulky solution. The switching resistive solution was adopted. As far as the choice of the switch is concerned, the need for good balancing capability and especially for high reliability leads to an automotive technology solution. In order to obtain a simple and reliable solution a protected FET (ProFET) [13] was used in parallel to each cell of the pack to drain current from the cells at the threshold of overvoltage (4.15 V). In overvoltage conditions the battery charge will continue without overcharging the cell

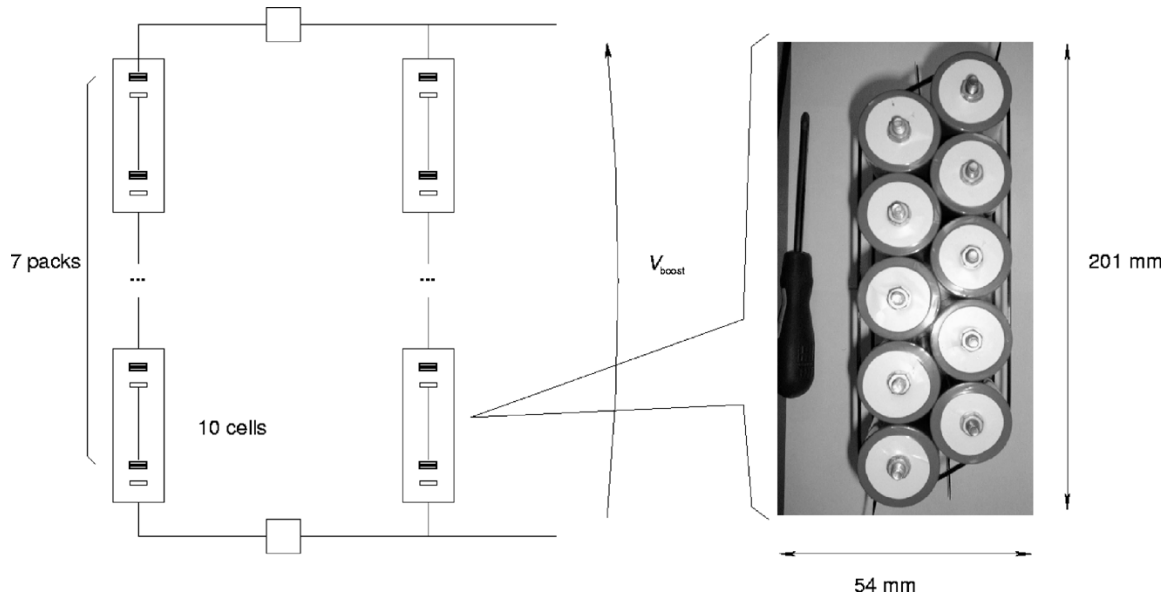


Fig. 1. Battery cells hierarchical structure.

TABLE II  
EQUALIZATION CIRCUIT CHARACTERISTICS

Method	Advantage	Disadvantage
Switched Capacitor	Simple Circuit Elements	Low equalizing capability
Variable Analog cell shunting	Good balancing capability. Constant voltage model.	Complex power electronics. Thermal management. Energy efficiency (90%).
Switched Resistive	Good Balance capability. Simple Electronics. Low power Requirements.	Thermal management. Energy efficiency (90%).
Switched Resistive Inductor/Trasf.	Energy efficiency (99%)	Mass. Cost. EMI.

because of the shunting operation performed by the ProFET. Battery charging will be stopped when the cell overvoltage monitoring circuit detects a voltage of about 4.25–4.3 V. The ProFET is a smart FET, which includes a high-side drive and is fully protected by embedded protection functions, thus, this solution greatly simplifies the equalization circuit. Table III reports ProFET current capabilities. A dedicated circuit for equalization purposes was designed for each cell inside the battery pack relying on ProFETs (see Fig. 2).

The choice of the components of the control circuit was driven by the need of low power consumption of the board (500 mW). Because of the large number of devices, they were placed on two faces in a four-layer printed circuit board (PCB). The conformation and the size of the board are related to the size of the battery pack composed of ten cells; in fact, the board is mounted on the battery pack, in order to reduce the volume. The size of the board is 201 mm  $\times$  54 mm (7.91  $\times$  2.12 in). SMT components were used for size and precision purposes.

The pads, which provide the voltage of each cell, were placed in order to reach the cell connectors by screwed bars for ease of assembly.

TABLE III  
ProFET CHARACTERISTICS

Nominal load current	3.1 A
Repetitive Short Circuit Current Limit	12 A

### III. BATTERY MANAGEMENT

Battery state can be achieved if battery state of charge (SoC) and battery state of health (SoH) can be accurately monitored [14].

A few experiments were made to define an accurate and reliable procedure for SoC detection. As already stated, batteries are one of the weakest parts of an EV. Limited autonomy and recharge facilities are some of the main drawbacks. Therefore, the full exploitation of the battery is a key element, and this requires an accurate knowledge of the actual SoC.

Accurate estimation of SoC is a complex task. To accomplish it, a few approaches are possible: circuit models, empirical models, statistical or artificial-intelligence-based models [8], [9], [7], [10]. Circuit models require much work for each type of battery and require nonlinear elements. Classical methods for SoC estimation include: measurements of the extracted charge, measurements of the battery internal impedance or

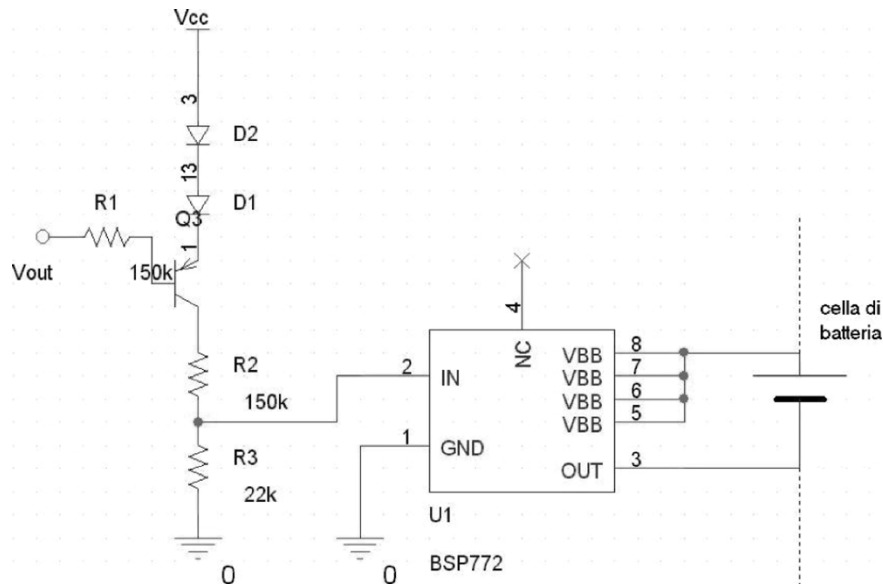
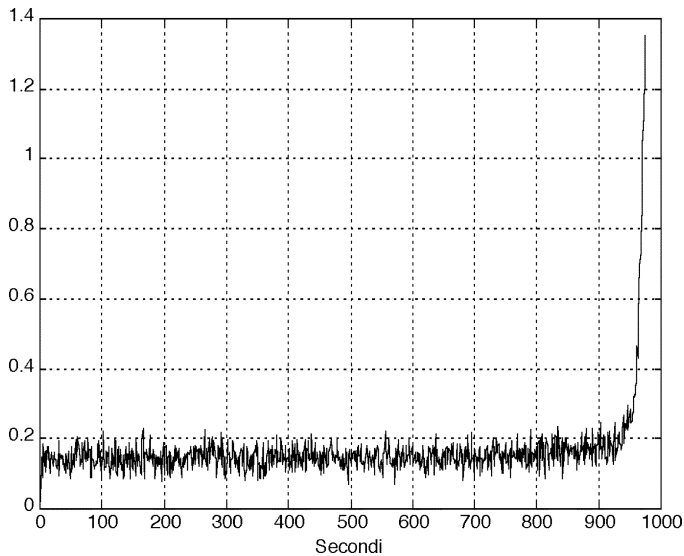


Fig. 2. Single-cell equalization circuit.

Fig. 3. 1.5-Ah battery cell  $R_i$  profile.

resistance, and measurements of the battery no-load voltage. Though none of these provides acceptable results, a hybrid method, including measurements of internal impedance or resistance ( $R_i$ ), extracted charge ( $Q_e$ ), and no-load voltage ( $fem$ ), can achieve a better estimation of SoC. Fig. 3 refers to a 1.5-Ah battery cell; it shows the  $R_i$  profile as a function of time: the profile is almost constant during battery discharge and it suddenly increases close to the end of discharge. This profile alone is not sufficient to evaluate the SoC. Fig. 4 refers to a 10-Ah battery cell; it shows a discharge profile as a function of time at constant discharge current, equal to the battery capacity.  $Q_e$  can be computed using this profile, however, this quantity is not sufficient to state SoC. The knowledge of the amount of energy that can be extracted from the battery is a key element in order to optimize system performance. This information can be retrieved starting from SoC only if battery discharge status is fully defined. A battery can be defined as being completely discharged when it cannot provide the power needed by the

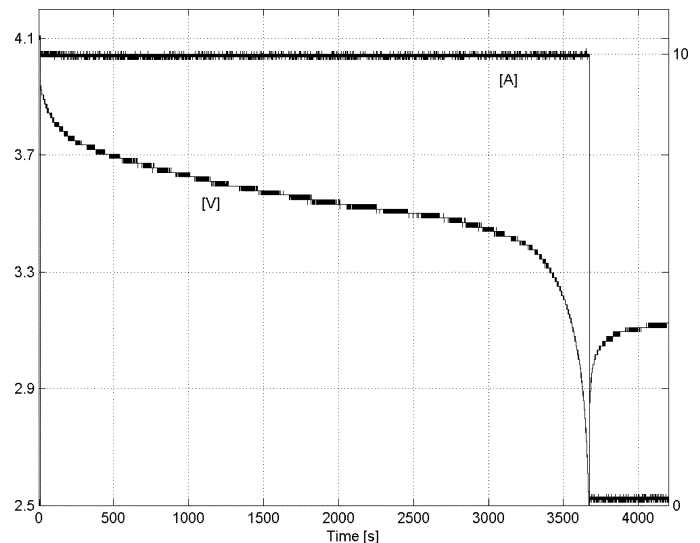


Fig. 4. 10 Ah battery cell discharge profile.

system it supplies. Therefore, an accurate estimation of SoC should be made only by fully discharging the battery. This procedure is impractical because of the large amount of time required. The authors' assumption is that SoC decreases linearly with time if discharge occurs with a periodical current profile. This simple approximation was then verified *a posteriori* by laboratory tests. Starting from this assumption, the authors propose a neural-network (NN)-based procedure that allows the estimation of battery SoC mapped as a function  $f$  of  $fem$ ,  $Q_e$ , and  $R_i$ .

The aim is to find a function  $f$  so that  $\text{SoC} = f(fem, Q_e, R_i)$ . As stated before  $f$  can be obtained from an analytical study of the physical and chemical behavior of batteries, or it can be mapped from empirical data. The latter approach turns out to be preferable, since it is simpler and often more efficient. In this paper, an empirical estimation of  $f$  was made, using an NN, which maps the input vector:  $fem$ ,  $Q_e$ ,  $R_i$  into the SoC [7], [10].

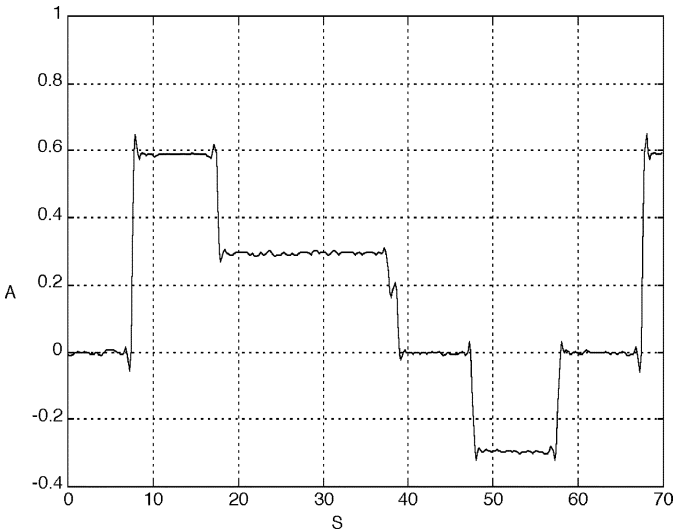


Fig. 5. Typical discharge current profile as a function of time for a single cell.

As usual, the NN estimation is more accurate if the training set is large and fully representative of different operating conditions. Therefore, the behavior of  $f$  was analyzed in several different conditions, performing several different discharge cycles. Specifically, the test setup must allow discharging the battery cell with a given current to measure cell voltage and current during discharge. Fig. 5 shows a current profile chosen according to the typical EV urban duty cycle for a single cell. The test setup for the experiments was made by a programmable current generator, a data-logger, and a host PC with IEEE-488 interface and suitable LabView software. Two graphical user interfaces (GUIs) were designed in LabView which allow us to specify the desired current profile during battery discharge, to set up the measurements, and to store collected data on the host PC. Starting from measured data (battery current and voltage during discharge) a MATLAB [12] script is used to produce the training set.  $Q_e$  is computed with the composite trapezoidal approximation from current sampling.  $R_i$  is computed measuring the voltage drop corresponding to a current variation. Finally,  $f_{em}$  was estimated directly as the voltage with no load in time intervals where the current is zero. The SoC values suitable for NN training are obtained in accordance with the previous assumption on cell discharge behavior.

The collected training data were used to train a two-layer NN with *tansig* activation function. The learning procedure is based on the Broyden, Fletcher, Goldfarb and Shanno (BFGS) algorithm [11], [12].

The trained NN was then used as a real-time estimator of the battery SoC. In order to validate the estimation results, different tests were performed changing the discharging conditions. Specifically, the current profile was varied during every validation test in order to prove the NN performance in operations close to the real ones. Each test was stopped after a consistent number of cycles, the battery was fully discharged, and the measure of the extracted charge was compared with the NN output. Two different Lithium-ion battery cells were used. As an example, Fig. 6 shows the battery SoC estimated by NN compared with the actual SoC measured during the discharge of a Lithium-ion battery. The curves are almost completely overlapped.

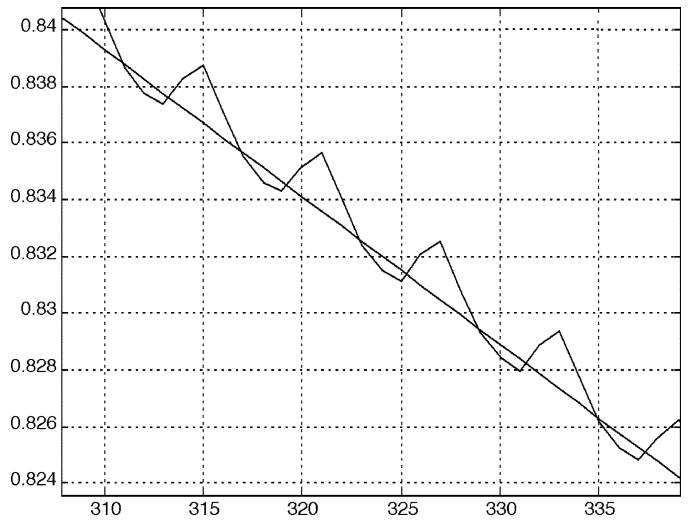


Fig. 6. Neural network estimation (light grey) compared with current SoC as a function of time cycles.



Fig. 7. Prototype battery pack.

Several discharge cycles were repeated with the described test setup, obtaining a good agreement between NN estimation and measured results, for different tests performed with different discharge current profiles.

The SoC information allows the tuning control strategy of the EV according to journey characteristics. This leads to the optimization of battery lifespan instead of useless performance in the case of an urban journey. The developed method is based on an NN estimator in order to comply with the nonlinear behavior of the battery, providing a simple and effective implementation. Experiments were made on different discharge profiles modeled on the typical urban EV duty cycle [15].

#### IV. EXPERIMENTAL RESULTS

In order to verify the design of battery management circuits shown in the previous sections a prototype battery pack was realized, including battery protection and SoC detection (see Fig. 7).

The realized battery pack includes detection of battery SoC allowing different control strategy depending on journey or

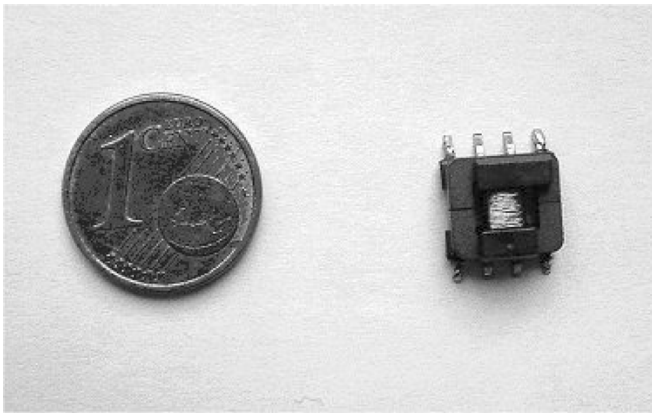


Fig. 8. Photograph of the switching transformer.

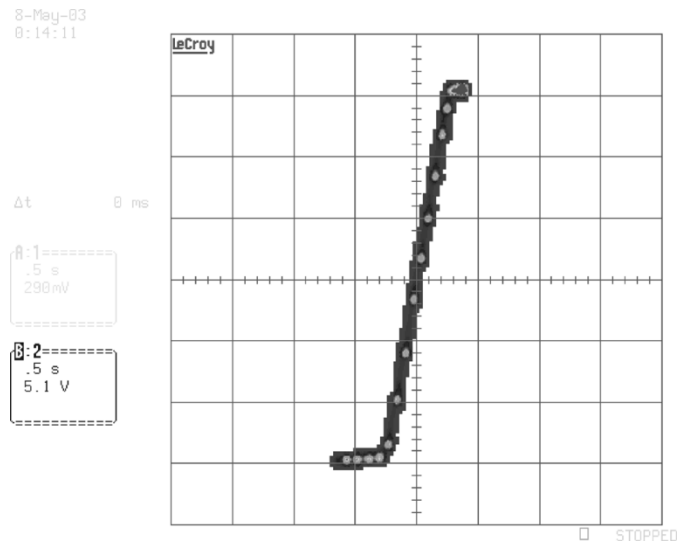


Fig. 10. Shunted current, cell voltage characteristic.

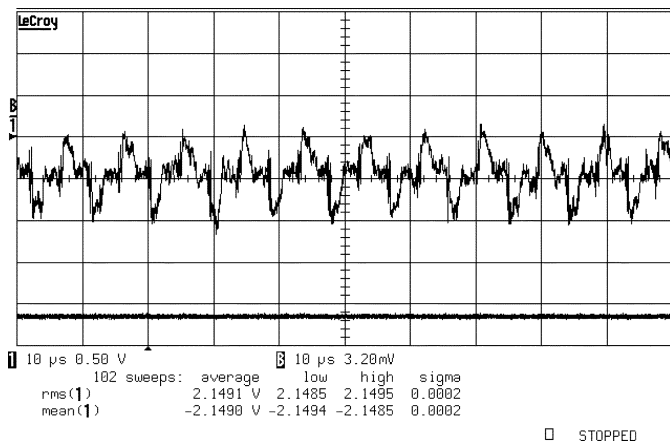


Fig. 9. Voltage reference output (black) and its ac ripple residual (light grey).

driver requirements. These battery packs will be used to supply a high-performance electric scooter [15]. The specifications of the electric scooter are: 6-kW motor; 5 kWh; 130 km of autonomy at 50 km/h.

In order to minimize battery consumption and to ensure proper operation of monitoring circuits even in the case of low cell voltage, the power supply is external. The voltage supply waveform is a trapezoidal wave 30 V peak to peak, at high frequency (100 kHz) [16], [17]. In order to obtain correct voltages for electronic components a suitable switching transformer was realized (see Fig. 8).

The switching transformer supplies a voltage doubler circuit and an ac/dc converter. Because of the required voltage resolution a low supply ripple is mandatory. The residual ripple at the output of the ac/dc converter at full load is about 50 mV peak to peak.

Fig. 9 reports the output of the voltage reference and the residual ac ripple. As previously stated, voltage reference stability is a key element for the accurate monitoring of the cell voltage.

The figures now cited show overvoltage and undervoltage circuits behavior. Specifically, Fig. 10 shows the drained current versus cell voltage characteristic. Fig. 11 shows overvoltage circuit behavior: if the cell voltage surpasses the threshold (4.15 V) the ProFET starts draining current and, eventually, when the proFET runs thermally and cell voltage rises to 4.25 V the monitoring output becomes low, stopping battery charge. The results shown in the figure are obtained using a programmable voltage

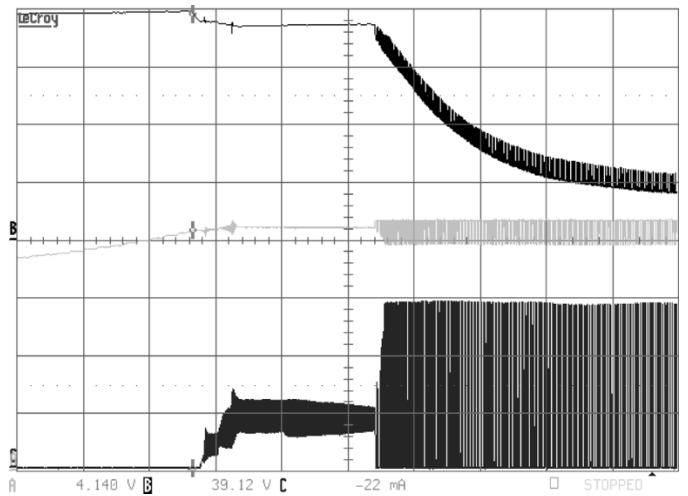


Fig. 11. ProFET current (top trace). Cell voltage (middle trace) overvoltage circuit output (bottom trace).

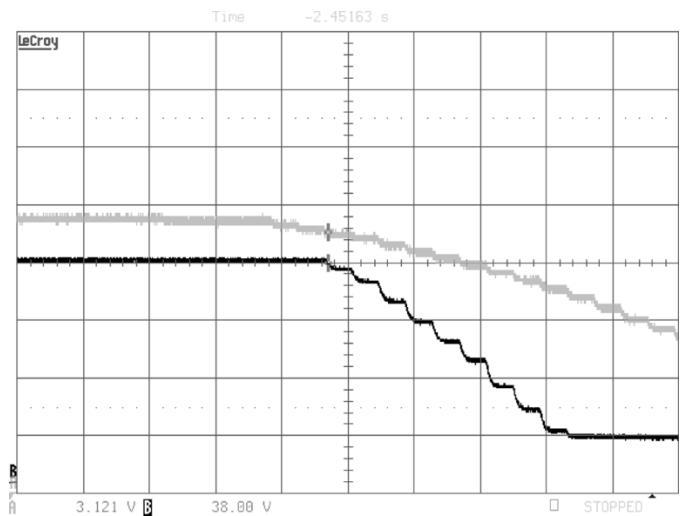


Fig. 12. Cell voltage (light gray trace) and undervoltage circuit output (black trace).

source to simulate battery behavior. Fig. 12 shows undervoltage monitoring.

As can be seen, when the cell voltage falls below 3.12 V the output of the undervoltage circuit starts to decrease down to a low level in correspondence to a cell voltage of 2.79 V, i.e., the lower threshold.

## V. CONCLUSION

A simple approach for protection and estimation of SoC of Li-ion batteries tailored for EV applications has been presented. The proposed estimation is based only on the measurement of electrical quantities like  $f_{em}$ ,  $Q_e$ , and  $R_i$ , which are usually available without introducing further invasive sensors. Electronic circuits for charge equalization, undervoltage and overvoltage monitoring, and temperature sensing were designed and implemented on a dedicated PCB. Their outputs drive motor control strategy according to journey characteristics. The implemented charge equalization strategy allows for obtaining the maximum energy storage also during vehicle braking operation. The proposed control board was embedded in a prototype electric scooter in order to increase its reliability and autonomy.

## REFERENCES

- [1] T. J. Miller, "Lithium-ion battery automotive applications and requirements," in *Proc. Seventeenth Annu. Battery Conf. Applications and Advances*, 2002, pp. 113–118.
- [2] Y. Nishi, K. Katayama, J. Shigetomi, and H. Horie, "The development of lithium-ion secondary battery systems for EV and HEV," in *Proc. Thirteenth Annu. Battery Conf. Applications and Advances*, 1998, pp. 31–36.
- [3] M. J. Isaacson, R. P. Hollandsworth, P. J. Giampaoli, F. A. Linkowsky, A. Salim, and V. L. Teofilo, "Advanced lithium-ion battery charger," in *Proc. Fifteenth Annu. Battery Conf. Applications and Advances*, 2000, pp. 193–198.
- [4] D. Salerno and R. Korsunsky, "Practical considerations in the design of lithium-ion battery protection systems," in *Proc. IEEE APEC'98*, vol. 2, 1998, pp. 700–707.
- [5] U. Koehler, F. J. Kruger, J. Kuempers, M. Maul, E. Niggemann, and H. H. Schoenfelder, "High performance nickel-metal hydride and lithium-ion batteries," in *Proc. IECEC'97*, vol. 1, Jul. 27–Aug. 1, 1997, pp. 93–98.
- [6] H. Tsukamoto, "High reliability lithium rechargeable batteries for specialties," *IEEE Aerosp. Electron. Syst. Mag.*, vol. 18, no. 1, pp. 21–23, Jan. 2003.
- [7] T. Yamazaki, K. Sakurai, and K. Muramoto, "Estimation of the residual capacity of sealed lead-acid batteries by neural network," in *Proc. IEEE PESC'98*, 1998, pp. 210–214.
- [8] O. Caumont, P. Le Moigne, C. Rombaut, X. Muneret, and P. Lenain, "Energy gauge for lead acid batteries in electric vehicles," *IEEE Trans. Energy Convers.*, vol. 15, no. 3, pp. 354–360, Sep. 2000.
- [9] T. Yanagihara and A. Kawamura, "Residual capacity estimation of sealed lead-acid batteries for electric vehicles," in *Proc. PCC Na-gaoka'97*, 1997, pp. 943–946.
- [10] J. Peng, Y. Chen, and R. Eberhart, "Battery pack state of charge estimator design using computational intelligence approaches," in *Proc. Fifteenth Annu. Battery Conf. Applications and Advances*, 2000, pp. 173–177.
- [11] T. Fukuda, "Theory and applications of neural networks for industrial control systems," *IEEE Trans. Ind. Electron.*, vol. 39, no. 6, pp. 472–489, Dec. 1992.
- [12] *MATLAB. Neural Networks Toolbox*, The MathWorks Inc., Natick, MA, 2004.
- [13] "BSP 772 T Smart Power High-Side-Switch," Infineon Technologies AG, Munich, Germany, 2004.
- [14] A. Affanni, A. Bellini, C. Concari, G. Franceschini, E. Lorenzani, and C. Tassoni, "EV battery state of charge: Neural network based estimation," in *Proc. IEEE IEMDC'03*, vol. 2, Madison, WI, Jun. 2003, pp. 684–688.
- [15] P. Casasso, A. Fratta, G. Giraudo, P. Guglielmi, M. Pastorelli, and A. Vagati, "High-performance electric scooter," in *Proc. PCIM'03*, Nuremberg, Germany, May 2003.
- [16] A. Fratta, P. Guglielmi, G. M. Pellegrino, and F. Villata, "DC-AC conversion strategy optimized for battery or fuel-cell-supplied AC motor drives," in *Proc. IEEE ISIE'00*, vol. 1, 2000, pp. 230–235.

- [17] P. Casasso, A. Fratta, G. Giraudo, P. Guglielmi, and F. Villata, "Feasibility, test and novel design of battery packs for EV scooter," in *Proc. IEEE IECON'03*, vol. 2, Nov. 2–6, 2003, pp. 1649–1654.



**Antonio Affanni** was born in Italy in 1977. He received the Master's degree in electronic engineering in 2003 from the University of Parma, Parma, Italy, where he is currently working toward the Ph.D. degree.

His current research interests include sensors for industrial applications and high-performance electric drives.



**Alberto Bellini** (S'96–M'04) was born in Italy in 1969. He received the Dr.Eng. degree in electrical engineering and the Ph.D. degree in computer science and electronics engineering from the University of Bologna, Bologna, Italy, in 1994 and 1998, respectively.

Since 1999, he has been with the University of Parma, Parma, Italy, where he is currently an Assistant Professor of Electrical Engineering. His research interests include power electronics, signal processing for audio and industrial applications, and diagnosis. He has authored or coauthored more than 70 papers and is the holder of three industrial patents.

electric drive design and 70 papers and is the holder of three industrial patents.



**Giovanni Franceschini** was born in Reggio Emilia, Italy, in 1960. He received the Master's degree in electronic engineering from the University of Bologna, Bologna, Italy.

In 1990, he joined, as an Assistant Professor, the Department of Information Technology, University of Parma, Parma, Italy, where he currently is an Associate Professor. His research interests include high-performance electric drives and diagnostic techniques for industrial electric systems. He has authored or coauthored more than 100 technical papers and is the holder of three industrial patents.

papers and is the holder of three industrial patents.



**Paolo Guglielmi** was born in Imperia, Italy, in 1970. He received the M.Sc. degree in electronic engineering and the Ph.D. degree in electrical engineering from the Politecnico di Torino, Turin, Italy, in 1996 and 2001, respectively.

In 1997, he joined the Department of Electrical Engineering, Politecnico di Torino, where he became a Researcher in 2002. His fields of interest are power electronics, high-performance servo drives, and computer-aided design of electrical machines. He has authored several papers published in technical journals

and conference proceedings.

Dr. Guglielmi is Registered Professional Engineer in Italy.



**Carla Tassoni** (SM'97) was born in Bologna, Italy, in 1942. She received the Master's degree in electrical engineering from the University of Bologna, Bologna, Italy, in 1966.

She joined the University of Bologna as an Assistant Professor and then became an Associate Professor of Electrical Machines in the Department of Electrical Engineering. She is currently a Full Professor of Electrical Engineering at the University of Parma, Parma, Italy. She has authored or coauthored more than 100 scientific papers and is the holder of an industrial patent. Her main research interests include the simulation and modeling of electric systems and applications of diagnostic techniques.

Prof. Tassoni is a Member of the European Consortium for Research on Condition Monitoring of Electric Systems and Drives (CRCM).